Prediction of Aerodynamic Characteristics in Upper Airways with Lateral Cephalograms

Xin Feng
University of Bergen
Yicheng Chen
Harbin Institute of Technology
Weihua Cai
Northeast Electric Power University
Stein Atle Lie
University of Bergen
Kristina Hellén-Halme
Malmö University
Xie-Qi Shi (xieqi.shi@uib.no)
University of Bergen

Research Article

Keywords: Lateral cephalogram, CBCT, Adenoids, Upper airway, Computational Fluid Dynamics

Posted Date: May 10th, 2021

DOI: https://doi.org/10.21203/rs.3.rs-494769/v1

Abstract

Background: The lateral cephalogram is a common imaging diagnostic test for adenoid hypertrophy (AH) in clinics. The study aims to investigate the aerodynamic characteristics within the upper airway (UA) by employing a computational fluid dynamics (CFD) simulation. Furthermore, airflow features are compared between subgroups according to the adenoidal nasopharyngeal (AN) ratios.

Methods: This retrospective study included thirty-five cases involving individuals aged 9-15 years who fulfilled the inclusion criteria of having both a lateral cephalogram and cone beam computed tomography (CBCT) imaging that covered the UA region. Based on the three-dimensional (3D) models of the UA segmented from the CBCT images, the aerodynamic characteristics at inspiration and expiration were simulated by the CFD method. The studied aerodynamic parameters were pressure drop ($\triangle P$), maximum midsagittal velocity (V_{ms}), maximum wall shear stress (P_{ws}), and minimum wall static pressure (P_w). The cases were divided into two subgroups: Group 1 was comprised of cases with an AN ratio < 0.6 and Group 2 with an AN ratio ≥ 0.6. The aerodynamic parameters were compared between the two groups.

Results: The maximum V_{ms} exhibits nearly 30% increases in Group 2 at both inspiration ($p = 0.013$) and expiration ($p = 0.045$) compared to Group 1. For the other aerodynamic parameters such as $\triangle P$, the maximum P_{ws}, and minimum P_w, no significant difference is found between the two groups.

Conclusions: The maximum V_{ms} is the most sensitive aerodynamic parameter for the groups of cases. An AN ratio of more than 0.6 measured on a lateral cephalogram may predict the noticeably increased maximum V_{ms}, which could assist clinicians in estimating the airflow features in the UA.

Background

Hans Wilhelm Meyer first described the clinical condition of nasal obstruction caused by adenoid hypertrophy (AH) in 1868 [1]. Recurrent or chronic upper airway (UA) infections, allergic inflammation, and immune response may lead to AH, one of the most common causes of UA obstruction in children and adolescents [2, 3]. Many studies have suggested that AH is related to cardiopulmonary complications, craniofacial growth, and obstructive sleep apnea [4–6]. The presence of AH causes a varying degree of nasopharyngeal obstruction, mouth breathing, and snoring, and it could affect craniofacial growth. A specific “adenoid face” is characteristic among AH patients who have a narrow and high maxillary arch, abnormal position of the tongue, and retrusion of the mandible [7]. Thus, early identification of the airflow alteration caused by AH in orthodontic patients is essential to avoid further complications. Currently, the nasendoscopy is considered the standard for clinically assessing the adenoid size on cooperative children [8].

Lateral cephalograms, cone beam computed tomography (CBCT), computed tomography (CT), and magnetic resonance imaging have been investigated to evaluate the size, shape, and location of the adenoid [9–12]. The adenoid size and patency of the surrounding nasopharynx could be presented in

terms of the absolute dimensions of adenoid thickness and nasopharyngeal width [13], percentage of adenoid-nasopharyngeal obstruction [10, 14], cross-sectional areas [12] and volumes [15] of the adenoid and nasopharynx. Among the radiological modalities, the lateral cephalogram has been widely applied in children and adolescents to depict and trace the skeletal structures and occlusion during the orthodontic treatment process. Since the presence of AH affects occlusion and craniofacial morphology [7, 16], adenoid assessment is an integral part of cephalometric analysis for this group of children.

The adenoid size and patency of the nasopharyngeal airway could also be depicted on a lateral cephalogram by looking at the adenoidal nasopharyngeal (AN) ratio [9]. The AN ratio was found to correlate significantly with the nasopharyngeal volume [17], clinical endoscopic examination [18], and symptoms of obstructive sleeping [19]. Feng et al. [17] investigated the AN ratios in relation to the 3D volumetric data and recommended using the AN ratio as an initial screening method to estimate the nasopharyngeal volumes of patients younger than 15 years old. An AN ratio of 0.6 is considered a threshold when suspecting AH, whereas an AN ratio value of more than 0.7 has been well accepted for indicating pathological AH, and an adenoidectomy may be suggested by clinicians after clinical assessment [20, 21]. Current diagnosis of AH is based on adenoid morphology; the ultimate effect of adenoid size on respiratory function in terms of airflow alteration is yet unclear.

Computational fluid dynamics (CFD) simulations may be the solution to further investigation into the relationship between UA morphology and airflow characteristics. CFD simulation is a well-established method for simulating the flow of gases or fluids and their interactions with the surrounding surfaces, as defined by boundary conditions. It has been widely used in the industry to predict the dynamic characteristics of the targeted flow. However, the application of CFD in dentistry was nevertheless sparse and had mainly been applied in evaluating the outcome of mandibular advancement devices in sleep-disordered breathing [22–24]. CFD has been accepted as an accurate and reliable method for associating the maxillofacial morphology and the UA's aerodynamic characteristics [22, 25, 26].

The study aims to investigate the aerodynamic characteristics within UA by employing CFD simulation. Furthermore, airflow features are compared between normal cases and cases suspected of having AH according to the AN ratios.

Methods

Sample size estimation

Maximum midsagittal velocity of the airflow in the upper airway is considered to be the primary outcome variable based on a previous study by Feng et al [27]. A sample size of 30 will be needed to ensure a 80% power to reject the null hypothesis at a significance level of 5%, assuming differences in maximum midsagittal velocity and its standard deviation is 0.7 m/s and 0.5 m/s between the cases with an AN ratio less than 0.6 and equal or more than 0.6, and the ratio between the two groups is 2:1.

Samples collection

This cross-sectional study is a subset of a longitudinal prospective study that was performed at Dalian Stomatological Hospital between 2015 - 2017, in which 2D and 3D image modalities were compared for tracing anatomic landmarks before and after orthodontic treatment. The study was approved by the regional ethics review boards in Dalian, China (DLKQLL201604) and Bergen, Norway (2018/1547 REK Vest). Informed consent was obtained from all patients or their legal guardians. The baseline images from 2015 were retrospectively collected and employed in the current study. The inclusion criteria were individuals aged 9 to 15 years who had had both a lateral cephalogram and CBCT scan examined within one week. For CBCT images, the field of view was required to cover the UA regions, including the nasal cavity, nasopharynx, and oropharynx. The exclusion criteria were severe maxillofacial abnormalities and previous surgery on skeletal and soft tissue related to respiration. In the present study, ninety-two cases were initially included. X.F previewed all the CBCT scans and lateral cephalograms. Fifty-seven cases were excluded, of which 53 did not cover the UA, 3 scans had motion artefact and 1 showed suboptimal patient positioning. Eventually, thirty-five cases were recruited. All the cases were divided into two groups: Group 1 with AN ratios < 0.6 (n=25) and Group 2 with AN ratios ≥ 0.6 (n=10).

Lateral cephalogram

The AN ratios were measured and calculated on the lateral cephalograms captured by a digital pan/ceph system (ORTHOPHOS XG 5; Sirona Dental Systems, Bensheim, Germany) at 73 kVp and 15 mA with exposure times of 9.4 seconds and a contrast resolution of 16-bit depth. A is a perpendicular distance between the point of maximal convexity of the adenoid to the anterior margin of the basiocciput. N is the distance between the posterosuperior edge of the hard palate and the anteroinferior edge of the spheno-occipital synchondrosis [9] (Figure 1).

CBCT scans

All CBCT scans were obtained by 3D eXam (KaVo, Biberach an der Riss, Germany). The following parameters were used: a field of view (FOV) of 16 × 13 cm, tube voltage of 120 kV, tube current of 5 mA, scanning time of 14.7 seconds, voxel size of 0.2 mm, and contrast resolution of 14-bit depth.

CFD simulation

The CBCT images were imported in the digital imaging and communications in medicine (DICOM) format to MIMICS software (MIMICS, Materialise, Belgium) for later analysis. 3D renderings of the CBCT scans were oriented with axial planes parallel to the Frankfurt horizontal plane; the midsagittal planes intersected the nasion and anterior nasal spine; and the coronal plane was adjusted to the level of the porions. For each case, a mask was reconstructed, making sure the integrity of UA displayed correctly.

CFD simulation was then conducted on the 3D model within the mask region. The superior boundary of the studied UA was defined as a vertical plane, in the nasal cavity, passing through the most posterior point of the middle turbinate, whereas the inferior boundary was a horizontal plane, in the pharynx, in line with the most anterior-inferior point of cervical vertebra 4. Each end of the boundary was extended by 20mm to avoid flow reversing during the simulating process. The inlet and outlet of UA were set on the extended planes. A surface model was then created according to the extended 3D model for mesh generation. We chose tetrahedral and prismatic cells to construct the main body and boundary layer of the UA mesh (ANSYS, Inc., Canonsburg, Pennsylvania). The SST κ-ω model was used to calculate the aerodynamic characteristics of UA by applying ANSYS Fluent (ANSYS, Inc., Canonsburg, Pennsylvania). The wall of the UA was defined as no-slip, stationary, and rigid. The temperature and density of air were set as fixed. At inspiration, the inlet was set with the pressure 0 Pa and the outlet at a flow rate of - 200 mL/s [28]. The corresponding values were - 200 mL/s and 0 Pa at inlet and outlet at expiration.

Data analyses

The aerodynamic parameters applied and computed throughout the CFD simulation are listed in Table 1. The pressure drop (△P) refers to the pressure difference between a vertical plane through the most posterior point of the middle turbinate and a horizontal plane through the tip of the epiglottis. Data were processed using IBM-SPSS, version 25.0 (IBM, New York, NY, USA). Significance was set at p-values less than 0.05. The assumption of normal distribution for all variables were tested. An independent-samples T test or Mann-Whitney U test was used for comparing each variable according to genders as well as groups. The Intraclass Correlation Coefficient (ICC) was applied for testing the intra- and inter-observer reliability on the selected ten cases using a random number generator.

Table 1

Description of the aerodynamic parameters evaluated applying the CFD simulation

Name	Unit	Definition
Maximum V_{ms}	m/s	The maximum velocity on the midsagittal plane
$\triangle P$	Pa	The pressure drop of airflow between the defined two planes
Maximum P_{ws}	Pa	The maximum lateral pressure of airflow acting on the UA wall
Minimum P_w	Pa	The minimum vertical pressure of airflow acting on the UA wall

Results

The mean age of cases was 12.03 ± 1.42 (13 females, 22 males). AN ratios ranged from 0.33 to 0.80 with a mean and standard deviation of 0.54 ± 0.15. The intra- and inter-observer reliability ranged between 0.872 and 0.997 for all measurements. We did not find any statistically significant difference between females and males in terms of AN ratio and aerodynamic parameters. Box plots of the four aerodynamic variables classified by the AN ratio at both inspiration and expiration are displayed in Fig. 2. The corresponding descriptive data of aerodynamic parameters for the two groups are listed in Table 2. The maximum V_{ms} in Group 2 exhibits a statistically significant increase of nearly 30% ($p < 0.05$) at both inspiration and expiration in contrast to Group 1. None of the other aerodynamic parameters, including $\triangle P$, maximum wall shear stress (P_{ws}), and minimum wall static pressure (P_w) were significantly different between the two groups at both inspiration and expiration.

Table 2
Comparison of the aerodynamic parameters between the two groups defined by the AN ratio 0.6.

	Group 1 (n = 25)		**Group 2 (n = 10)**		**Group 1 *Vs* Group 2**
	Mean	SD	Mean	SD	*p* value
Inspiration					
△P	-4.38	2.15	-4.65	2.18	0.373[a]
Maximum V_{ms}	2.36	0.46	3.04	0.80	**0.013**[a]
Maximum P_{ws}	2.50	5.14	0.93	0.54	0.190[b]
Minimum P_w	-11.18	5.09	-13.14	6.97	0.115[b]
Expiration					
△P	3.59	2.87	3.60	2.15	0.494[a]
Maximum V_{ms}	2.22	0.94	2.92	1.20	**0.045**[b]
Maximum P_{ws}	1.64	1.82	1.13	0.84	0.440[b]
Minimum P_w	-11.67	4.97	-13.67	5.87	0.157[a]

Group 1 consisted of the cases with AN ratio less than the 0.6 whereas Group 2 consisted of the cases with AN ratio equal or more than 0.6.

[a] Independent samples T test (one-tailed), [b] Mann-Whitney U test (one-tailed).

Discussion

The present study bridges UA morphology in terms of AN ratio and UA function regarding aerodynamic characteristics by applying CFD simulation. It also provides scientific evidence showing that clinicians could use a simple profile x-ray to estimate airflow alteration in the UA. Based on our results, the aerodynamic characteristics of the maximum V_{ms} significantly increased at both inspiration and expiration on cases with an AN ratio of more than 0.6. The relationship between UA's morphology and aerodynamics can be explained by the Bernoulli effect [29], which states that when a fluid flowing through a tube with varying diameters passes through a narrowing region, an increase in the speed of the fluid coincides with a decrease in pressure. Wakayama et al. reported that both maximum velocity and pressure drop at inspiration could be used to identify the nasal obstruction cases from controls [30]. In the present study, a significant increase was only observed in terms of maximum V_{ms} in Group 2 implying that the maximum V_{ms} is the most sensitive aerodynamic parameter associated with morphological changes within the upper airway [31].

We demonstrated that the AN ratio is associated with the nasopharyngeal volume in a previous study [17]. In the present study, we found that an AN ratio of more than 0.6 could indicate significant changes in airflow features in terms of the maximum V_{ms}. CFD simulation may be applied as a diagnostic tool to reveal the aerodynamic characteristics within the UA, making the airflow passing through the UA visible. Currently, the application of CFD in medicine and dentistry is still in the exploration stage of scientific research. To perform CFD on a large number of cases is challenging since it is highly dependent on the skillfulness of the operator; the simulation procedure is complicated and time-consuming. This may explain why the available CFD research in medicine consists mostly of case reports or a limited number of cases.

As compared to medical CT, CBCT is more cost-effective and has demonstrated a lower radiation dose [32]. However, we must keep in mind that CBCT scans have higher radiation doses than conventional 2D images [33]. In the current study we utilised the readily available imaging material and applied CFD simulation to investigate the airflow characteristics of these specific groups of cases. It keeps in line with the statement by the American Association of Orthodontists that “The airway and surrounding structures, specifically the adenoids in children, should be evaluated, if radiographic records are taken for orthodontic purposes” [34]. Lateral cephalograms are the most commonly performed radiographic examination, which is usually readily available among patients who start to undergo orthodontic treatment. From the perspective of morphological changes, the AN ratio on a lateral cephalogram may be applied as a useful screening method for estimating the nasopharyngeal volume [17]. The present study reinforces the impact of the AN ratio by its association with airflow features. As the AH may lead to maxillofacial dysmorphisms, multidisciplinary collaboration between orthodontists and otolaryngologists is the key to successful treatment for each individual [35] [36]. Based on our result, when the AN ratio is more than 0.6, a noticeable increase in airflow velocity (30%) is observed. Consequently, we may speculate alterations in breathing habits to overcome the nasal obstruction for this group of cases, such as mouth breathing. More prospective clinical studies are warranted to investigate the association between UA morphology, respiratory function, and clinical symptoms to better manage children with AH.

Conclusion

The maximum V_{ms} is the most sensitive aerodynamic parameter for the groups of participants. An AN ratio of more than 0.6 measured on a lateral cephalogram may predict the noticeably increased maximum V_{ms}, which could assist clinicians in estimating the airflow features in the UA.

Declarations

Ethics approval and consent to participate

The study was approved by the regional ethics review boards in Dalian, China (DLKQLL201604) and in Bergen, Norway (2018/1547 REK Vest). Informed consent was obtained from all participants or their legal guardians.

Consent for publication

Not applicable as there are no participants' identifiable data, picture or illustrations that require consent to publish in this manuscript.

Availability of data and materials

All data used and/or analysed during the current study are available from the corresponding author on reasonable request.

Competing interests

The authors declare that they have no competing interest.

Funding

This work was supported by grants provided by Dalian Medical Science Project, China (No. 1611079) as well as grants provided by University of Bergen, Norway (SPIRE project). The funding body was not involved in the study design, data collection, data analysis, or interpretation of data, or in writing the manuscript.

Author's contributions

X. Feng contributed to design, data acquisition, image segmentation, CFD simulation, and interpretation, drafted and critically revised the manuscript. Y.C. Chen contributed to the study design and supervised the CFD simulation process. W.H.Cai contributed to conception and design with respect to CFD simulation. S. A. Lie contributed to statistical analysis. K. Hellén-Halme contributed to conception, design, and supervised manuscript writing. X-Q Shi contributed to conception, design, data interpretation, and critically revised the manuscript. All authors commented on all drafts of the manuscript. All authors read and approved the final manuscript.

Acknowledgements

Not applicable

Conflicts of Interest

Xin Feng, Yicheng Chen,Weihua Cai, Stein Atle Lie, Kristina Hellén-Halme, and Xie-Qi Shi declare that they have no conflicts of interest.

Human rights

All procedures were in accordance with the ethical standards of the responsible committee on human experimentation (institutional and national) and with the Helsinki Declaration of 1964 and later versions. Informed consent was obtained from all study participants.

References

1. Meyer HW: Om adenoid Vegetationer Nasesvaelgrummet. Hospitalstidende 1868, 11:177-181.
2. Brambilla I, Pusateri A, Pagella F, Caimmi D, Caimmi S, Licari A, Barberi S, Castellazzi AM, Marseglia GL: Adenoids in children: Advances in immunology, diagnosis, and surgery. Clinical anatomy (New York, NY) 2014, 27(3):346-352.
3. Pagella F, De Amici M, Pusateri A, Tinelli G, Matti E, Benazzo M, Licari A, Nigrisoli S, Quaglini S, Ciprandi G *et al*: Adenoids and clinical symptoms: Epidemiology of a cohort of 795 pediatric patients. Int J Pediatr Otorhinolaryngol 2015, 79(12):2137-2141.
4. Krasny M, Wysocki J, Zadurska M, Skarzynski PH: Relative nasopharyngeal patency index as possible objective indication for adenoidectomy in children with orthodontic problems. Int J Pediatr Otorhinolaryngol 2011, 75(2):250-255.
5. Tatlipinar A, Biteker M, Meric K, Bayraktar GI, Tekkesin AI, Gokceer T: Adenotonsillar hypertrophy: correlation between obstruction types and cardiopulmonary complications. Laryngoscope 2012, 122(3):676-680.
6. Brooks LJ, Stephens BM, Bacevice AM: Adenoid size is related to severity but not the number of episodes of obstructive apnea in children. J Pediatr 1998, 132(4):682-686.
7. Koca CF, Erdem T, Bayındır T: The effect of adenoid hypertrophy on maxillofacial development: an objective photographic analysis. J Otolaryngol Head Neck Surg 2016, 45(1):48.
8. Kindermann CA, Roithmann R, Neto JFL: Sensitivity and specificity of nasal flexible fiberoptic endoscopy in the diagnosis of adenoid hypertrophy in children. International Journal of Pediatric Otorhinolaryngology 2008, 72(1):63-67.
9. Fujioka M, Young LW, Girdany BR: Radiographic evaluation of adenoidal size in children: adenoidal-nasopharyngeal ratio. AJR American journal of roentgenology 1979, 133(3):401-404.
10. Major MP, Witmans M, El-Hakim H, Major PW, Flores-Mir C: Agreement between cone-beam computed tomography and nasoendoscopy evaluations of adenoid hypertrophy. Am J Orthod Dentofacial Orthop 2014, 146(4):451-459.
11. Kapusuz Z, Ozkırış M, Okur A, Saydam L: The prevalence of adenoid hypertrophy in adults in a rural area of Turkey. Kulak Burun Bogaz Ihtis Derg 2012, 22(4):225-227.

12. Zeng G, Teng Y, Zhu J, Zhu D, Yang B, Hu L, Chen M, Fu X: Clinical application of MRI-respiratory gating technology in the evaluation of children with obstructive sleep apnea hypopnea syndrome. Medicine (Baltimore) 2018, 97(4):e9680.
13. Chiari S, Romsdorfer P, Swoboda H, Bantleon HP, Freudenthaler J: Effects of rapid maxillary expansion on the airways and ears--a pilot study. Eur J Orthod 2009, 31(2):135-141.
14. Bitar MA, Birjawi G, Youssef M, Fuleihan N: How frequent is adenoid obstruction? Impact on the diagnostic approach. Pediatrics international : official journal of the Japan Pediatric Society 2009, 51(4):478-483.
15. Schwab RJ, Kim C, Bagchi S, Keenan BT, Comyn FL, Wang S, Tapia IE, Huang S, Traylor J, Torigian DA *et al*: Understanding the anatomic basis for obstructive sleep apnea syndrome in adolescents. American journal of respiratory and critical care medicine 2015, 191(11):1295-1309.
16. Pawłowska-Seredyńska K, Umławska W, Resler K, Morawska-Kochman M, Pazdro-Zastawny K, Kręcicki T: Craniofacial proportions in children with adenoid or adenotonsillar hypertrophy are related to disease duration and nasopharyngeal obstruction. Int J Pediatr Otorhinolaryngol 2020, 132:109911.
17. Feng X, Li G, Qu Z, Liu L, Nasstrom K, Shi XQ: Comparative analysis of upper airway volume with lateral cephalograms and cone-beam computed tomography. Am J Orthod Dentofacial Orthop 2015, 147(2):197-204.
18. Caylakli F, Hizal E, Yilmaz I, Yilmazer C: Correlation between adenoid-nasopharynx ratio and endoscopic examination of adenoid hypertrophy: a blind, prospective clinical study. Int J Pediatr Otorhinolaryngol 2009, 73(11):1532-1535.
19. Tatlıpınar A, Biteker M, Meriç K, Bayraktar G, Tekkeşin A, Gökçeer T: Adenotonsillar hypertrophy: correlation between obstruction types and cardiopulmonary complications. Laryngoscope 2012, 122(3):676-680.
20. Elwany S: The adenoidal-nasopharyngeal ratio (AN ratio). Its validity in selecting children for adenoidectomy. J Laryngol Otol 1987, 101(6):569-573.
21. Ungkanont K, Damrongsak S: Effect of adenoidectomy in children with complex problems of rhinosinusitis and associated diseases. Int J Pediatr Otorhinolaryngol 2004, 68(4):447-451.
22. De Backer JW, Vanderveken OM, Vos WG, Devolder A, Verhulst SL, Verbraecken JA, Parizel PM, Braem MJ, Van de Heyning PH, De Backer WA: Functional imaging using computational fluid dynamics to predict treatment success of mandibular advancement devices in sleep-disordered breathing. J Biomech 2007, 40(16):3708-3714.
23. Zhao M, Barber T, Cistulli PA, Sutherland K, Rosengarten G: Simulation of upper airway occlusion without and with mandibular advancement in obstructive sleep apnea using fluid-structure interaction. J Biomech 2013, 46(15):2586-2592.
24. Martínez A, Muñiz AL, Soudah E, Calvo J, Suárez AÁ, Cobo J, Cobo T: Physiological and geometrical effects in the upper airways with and without mandibular advance device for sleep apnea treatment. Scientific reports 2020, 10(1):5322-5322.

25. Zhao M, Barber T, Cistulli P, Sutherland K, Rosengarten G: Computational fluid dynamics for the assessment of upper airway response to oral appliance treatment in obstructive sleep apnea. J Biomech 2013, 46(1):142-150.
26. Van Holsbeke C, De Backer J, Vos W, Verdonck P, Van Ransbeeck P, Claessens T, Braem M, Vanderveken O, De Backer W: Anatomical and functional changes in the upper airways of sleep apnea patients due to mandibular repositioning: a large scale study. J Biomech 2011, 44(3):442-449.
27. Feng X, Chen Y, Hellén-Halme K, Cai W, Shi X-Q: The effect of rapid maxillary expansion on the upper airway's aerodynamic characteristics. BMC Oral Health 2021, 21(1):123.
28. Iwasaki T, Saitoh I, Takemoto Y, Inada E, Kanomi R, Hayasaki H, Yamasaki Y: Improvement of nasal airway ventilation after rapid maxillary expansion evaluated with computational fluid dynamics. Am J Orthod Dentofacial Orthop 2012, 141(3):269-278.
29. Weese J, Lungu A, Peters J, Weber FM, Waechter-Stehle I, Hose DR: CFD- and Bernoulli-based pressure drop estimates: A comparison using patient anatomies from heart and aortic valve segmentation of CT images. Med Phys 2017, 44(6):2281-2292.
30. Wakayama T, Suzuki M, Tanuma T: Effect of Nasal Obstruction on Continuous Positive Airway Pressure Treatment: Computational Fluid Dynamics Analyses. PLoS One 2016, 11(3):e0150951.
31. Yanagisawa-Minami A, Sugiyama T, Iwasaki T, Yamasaki Y: Primary site identification in children with obstructive sleep apnea by computational fluid dynamics analysis of the upper airway. Journal of Clinical Sleep Medicine 2020, 16(3):431-439.
32. Ludlow JB, Ivanovic M: Comparative dosimetry of dental CBCT devices and 64-slice CT for oral and maxillofacial radiology. Oral surgery, oral medicine, oral pathology, oral radiology, and endodontics 2008, 106(1):106-114.
33. Kadesjö N, Lynds R, Nilsson M, Shi XQ: Radiation dose from X-ray examinations of impacted canines: cone beam CT vs two-dimensional imaging. Dentomaxillofac Radiol 2018, 47(3):20170305.
34. Behrents RG, Shelgikar AV, Conley RS, Flores-Mir C, Hans M, Levine M, McNamara JA, Palomo JM, Pliska B, Stockstill JW *et al*: Obstructive sleep apnea and orthodontics: An American Association of Orthodontists White Paper. Am J Orthod Dentofacial Orthop 2019, 156(1):13-28.e11.
35. Villa MP, Castaldo R, Miano S, Paolino MC, Vitelli O, Tabarrini A, Mazzotta AR, Cecili M, Barreto M: Adenotonsillectomy and orthodontic therapy in pediatric obstructive sleep apnea. Sleep Breath 2014, 18(3):533-539.
36. Huang YS, Guilleminault C: Pediatric Obstructive Sleep Apnea: Where Do We Stand? Advances in oto-rhino-laryngology 2017, 80:136-144.

Figures

Figure 1

Calculating the adenoidal nasopharyngeal (AN) ratio on a lateral cephalogram. A, Perpendicular distance between maximum convexity of the adenoid shadow and the anterior margin of the basiocciput. N, Distance between the posterosuperior edge of the hard palate and the anteroinferior edge of the spheno-occipital synchondrosis.

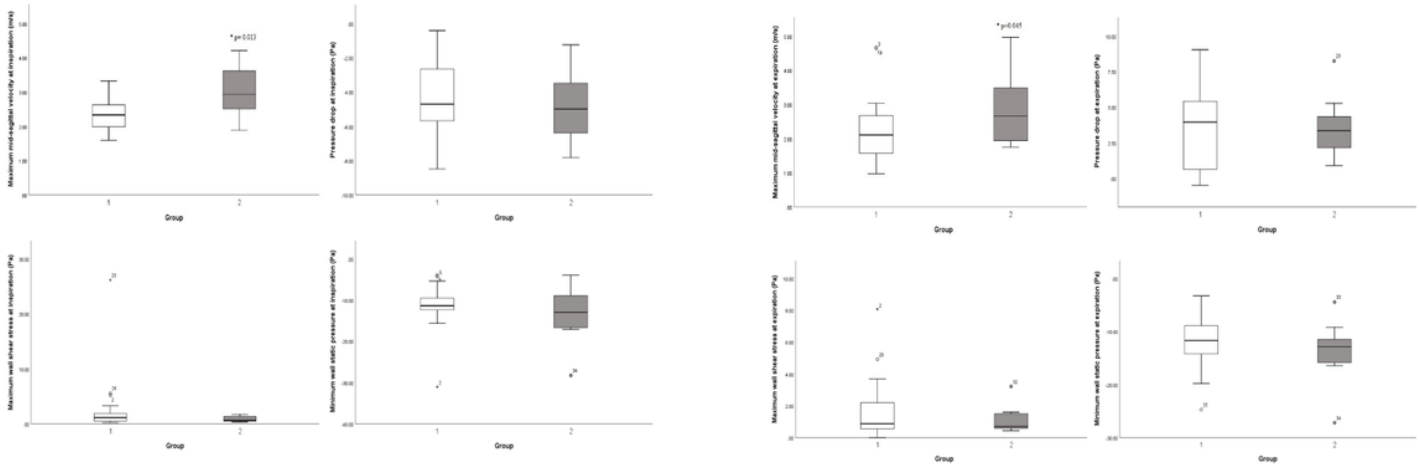

Figure 2

Comparison between the two groups in terms of four aerodynamic parameters at inspiration (a) and expiration (b).

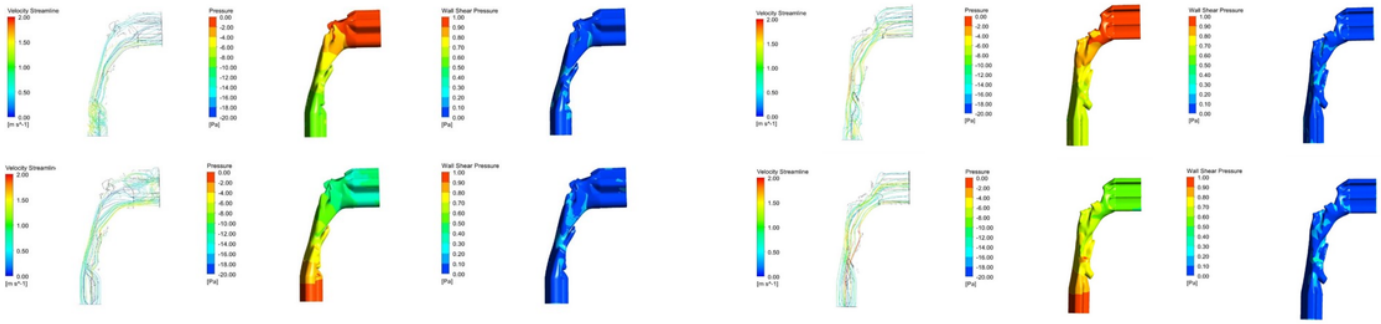

Figure 3

Illustration of the airflow feature in two typical cases with an AN ratio of 0.40 (a) and 0.73 (b), during inspiration (the up images) and expiration (the down images), respectively. In the case of an AN ratio of 0.40, the ΔP, Maximum Vms, Maximum Pws and Minimum Pw is -7.17, 1.95, 0.39, and -10.75 at inspiration and 7.50, 1.62, 1.44, and -14.97 at expiration. However, in the case of an AN ratio of 0.73, the corresponding values are -3.48, 3.62, 1.41, and -17.06 at inspiration and 5.29, 1.94, 0.59, and -12.88 at expiration.